

BATTERED AND BURNED: AN INVESTIGATION INTO THE
IDENTIFICATION OF BLUNT FORCE TRAUMA
FRACTURES TO THE RIBS IN
BURNED REMAINS

THESIS

Presented to the Graduate Council of
Texas State University-San Marcos
in Partial Fulfillment
of the Requirements

for the Degree

Master of ARTS

by

Adam H. Richard, B.S.

San Marcos, Texas
May 2007

COPYRIGHT

by

Adam Holtan Richard

2007

ACKNOWLEDGEMENTS

I would like to thank a number of people without whom this thesis would not have been possible. First, I would like to thank my thesis committee, particularly Dr. Melbye, for finding the time to provide both insight and guidance toward the completion of this project. Thank you to Dr. Mark Bing, David Brinsko, and Cheryl King for their generosity in allowing me to utilize the Katy Rehabilitation Hospital's brand new x-ray equipment. Thank you also to Stacy Schaefer and Corey Cromartie of Bluebonnet Pet Crematory for making themselves and their furnaces available for this research. I would also like to thank Dr. Grady Early for his unyielding support of the forensic anthropology program at Texas State University-San Marcos. Furthermore, I would like to extend a special thanks to my fellow graduate students. Words cannot express the importance that each of you has had in making a small-town Iowa boy feel at home when home is so far away. I will treasure the time we have spent together for the rest of my days. Finally, I wish to thank my family and friends for their continued support. It is comforting to know that, no matter where life may take me, I will always have someone on my side.

This manuscript was submitted on April 4, 2007.

TABLE OF CONTENTS

	Page
LIST OF TABLES.....	vi
LIST OF FIGURES.....	vii
CHAPTER	
1. BACKGROUND AND LITERATURE REVIEW	1
Physical Structure of Bone.....	2
General Fracture Mechanics of Bone.....	3
Fracturing in Ribs.....	5
Effects of Burning on Bone	7
Identification of Trauma in Burned Remains	9
Implications for Analyzing Blunt Trauma in Burned Ribs.....	12
2. MATERIALS AND METHODS	15
3. RESULTS	22
Control Group	23
Experimental Group.....	28
4. DISCUSSION	35
APPENDIX A: TIME AND TEMPERATURE DATA FOR BURN EVENTS	43
APPENDIX B: RAW DATA.....	44
APPENDIX C: VISUAL ATLAS OF FRACTURE CHARACTERISTICS	52
REFERENCES CITED.....	56

LIST OF TABLES

Table	Page
1. Frequency Table for Fracture Color in the Control Group	23
2. Frequency Table for Fracture Angle in the Control Group	25
3. Frequency Table for Fracture Line in the Control Group	26
4. Condensed Frequency Table for Fracture Line in the Control Group	26
5. Frequency Table for Fracture Edge in the Control Group	27
6. Frequency Table for Fracture Depth in the Control Group	28
7. Condensed Frequency Table for Fracture Depth in the Control Group	28
8. Frequency Table for Fracture Color in the Experimental Group	29
9. Frequency Table for Fracture Angle in the Experimental Group	30
10. Condensed Frequency Table for Fracture Angle in the Experimental Group	31
11. Frequency Table for Fracture Line in the Experimental Group	32
12. Frequency Table for Fracture Edge in the Experimental Group	32
13. Frequency Table for Fracture Depth in the Experimental Group	34
14. Condensed Frequency Table for Fracture Depth in the Experimental Group	34

LIST OF FIGURES

Figure	Page
1. Method Used to Inflict Blunt Force Trauma	16
2. Ribs Being Removed from the Furnace	17
3. Exposure of Trabecular Bone Around a Transverse Blunt Force Fracture	39
4. Warped Splinter of Bone from a Crushing Fracture.....	40

CHAPTER 1

BACKGROUND AND LITERATURE REVIEW

Criminals often go to great lengths to destroy evidence of their crimes. Of particular interest to forensic anthropologists is the disposal of the bodies of victims. Occasionally, this disposal process includes the burning of the victim's body in the hopes of obscuring the victim's identity or eliminating evidence of foul play. In response to this latter situation, many forensic anthropologists have begun researching the potential for identifying signs of perimortem trauma among burned remains (Bohnert et al. 1997, de Gruchy and Rogers 2002, Herrmann and Bennett 1999, Jackson 2005, Pope and Smith 2004). These studies have included examinations of the effects that burning has on a variety of bones as well as how to distinguish between heat fracturing and sharp, blunt, or projectile trauma. However, most of these studies have focused on cranial or long bone trauma with little attention given to the thoracic region. With that in mind, the intent of this study is to examine fracture patterns resulting from blunt force trauma to the ribs of *Sus scrofa* in both burned and unburned remains. The primary goal of this research, therefore, is to distinguish fracture patterns that

are the result of heat fracturing and post-burn manipulation from those that are the result of blunt force trauma.

Physical Structure of Bone

The majority of bones in the human body are composed of two types of bony tissue: cortical and trabecular. Cortical bone is the dense layer of bony tissue that comprises the surface of a bone. This tissue encompasses the underlying trabecular bone that is far more porous and spongy than the surrounding cortical bone. The relative ability of these two types of bone to resist both stress and strain factors are dependent upon different circumstances, but any calculation of the durability of a bone is contingent upon a composite of the physical properties of both types of bony tissue. The ability of cortical bone to resist stress and strain is largely dependent on the direction that the force is being applied relative to the orientation of the tissue's microstructures (Hipp and Hayes 1998). Cortical bone has been found to be much stronger when force is applied in the longitudinal direction than when it is applied transversely to the microstructural orientation. The strength of trabecular bone, on the other hand, is predominantly a factor of the relative density of the trabecular tissue in question (Hipp and Hayes 1998).

Microscopically, cortical bone is composed of a number of related features. As a bone grows in thickness, concentric rings of lamellar bone are laid

down in a fashion similar to tree rings. This process can occur quite rapidly, resulting in the inclusion of tiny blood vessels within the lamellar bone; these non-Haversian canals can be distinguished microscopically by the fact that the lamellar layers gradually bend around them without interruption (Kerley 1965). Haversian canals are formed by the action of osteoclasts eating through lamellar bone to make room for new blood vessels. These canals are characterized by the presence of concentric rings of secondary lamellar bone surrounding the canal as a result of remodeling; the structure formed by this secondary remodeling of bone is known as an osteon (Kerley 1965). Because the canals that form the center of each osteon are created longitudinally within the cortical bone, the resulting structure of these osteons is also oriented longitudinally.

General Fracture Mechanics of Bone

Hipp and Hayes (1998) identify four general types of fractures occurring in cylindrical bones. Each of these fracture types is associated with the application of a different form of force. When tension is applied to a tubular bone by pulling both ends of the bone in opposite directions, the resulting fracture occurs roughly perpendicular to the plane in which the force was applied. One possible explanation for this fracture behavior is related to the way in which bone grows. As a bone grows in length, layer upon layer of new growth is laid down effectively resulting in a stack of growth rings. This process

is visually evident in cases where growth is temporarily arrested, such as in the case of Harris Lines. Bonfield and Li (1966) suggest that internally these rings would be more structurally sound than the interfacial regions between adjacent rings. Consequently, when tension is applied, these weaker interfacial regions give way first and result in a transverse fracture pattern. However, if compression force is applied to both ends of a bone, an oblique fracture will occur at approximately a 45 degree angle to the plane of force (Hipp and Hayes 1998). When bending force is applied to a cylindrical bone, the side of the bone under tension will fracture transversely to the plane of force while the side undergoing compression will typically suffer from two oblique fractures. This fracture pattern is known as a butterfly fracture. Finally, when torsion is applied to a tubular bone, the resulting fracture occurs in a spiral around the circumference of the bone (Hipp and Hayes 1998).

Microscopic analysis of fractures reveals that they have a tendency to divert around osteons when undergoing slow propagation, testifying to the weaker bond between interosteon lamellae (Piekarski 1970). When such fractures do pass through the Haversian canal at the center of an osteon, the effective result is a blunting of the fracture tip that causes a dispersal of the stress over a greater area. This dispersal requires a greater level of stress for continued propagation of the fracture and may result in the termination of said fracture.

When viewed in profile with a scanning electron microscope, these slow-propagating fractures appear as Haversian pull-outs in which individual osteons can be seen to have pulled away from one another. The mechanics of this fracture morphology are related to cortical bone's similarity to a fiber-reinforced material. This type of "pull-out" fracture occurs when the matrix between fibers undergoes failure. On the other hand, when rapid fracture propagation occurs in cortical bone, it responds like a fiber-reinforced material undergoing tensile failure. In this instance, the fracture occurs in essentially one plane across all intervening microstructures with no evidence of Haversian pull-outs.

Fracturing in Ribs

Due to their unique morphology, ribs can undergo a significant amount of bending before fracturing; this may be part of the reason for the prevalence of "greenstick fractures" that commonly occur on ribs (Galloway 1999). Given the propensity for bending in ribs, it seems reasonable to expect that they will frequently experience the butterfly fracture pattern described by Hipp and Hayes (1998). However, when compression of the thoracic cage or impact from a blunt object is strong enough to fracture a rib, the side undergoing compression (i.e., the exterior surface) has been observed to suffer failure before the side under tension (i.e., the interior surface) in certain instances during controlled experiments (Daegling 2006). This finding is contradictory to experiments

conducted on long bones during which specimens subjected to bending forces always fractured on the side experiencing tension first. Daegling's (2006) results indicate that ribs fail to conform to the principles of biomechanical beam theory, and therefore, require further investigation to determine the exact mechanical principles under which they experience fracturing.

Fractures resulting from blunt force trauma to the thoracic cage are most commonly found on the lower ribs, while fractures of the upper ribs, particularly the first rib, typically result from the application of extreme force (Tomczak and Buikstra 1999). Rib fractures typically come in two morphological varieties: transverse and oblique (Galloway 1999). Transverse fractures tend to be more common and usually result from direct blunt force trauma to the thoracic cage. Oblique fractures, on the other hand, are typically associated with crushing or bending, often from a fall or car accident, and occur predominantly on the lateral curvature of the ribs. These lateral fractures are the direct result of anterior-posterior compression of the thoracic cage (DiMaio and DiMaio 2001). When compression occurs in the opposite direction (posterior-anteriorly), the resulting fractures tend to congregate near the spinal column. In contrast, lateral compression produces fractures near both the spinal and sternal ends of the rib.

Effects of Burning on Bone

One of the only early studies on the effects that burning has on bone structure (Binford 1963) involved attempts to determine if macroscopic differences could be identified among bones that had been burned with flesh still adhering, bones that had recently been macerated, and dry bone. Based on experimental results using human and monkey remains, Binford (1963) concluded that burning dry bone typically results in longitudinal fracturing with some incidental angular cracking. The burning of fleshed and recently macerated bone, on the other hand, results in deep transverse fracturing, often with a curved appearance, and frequent warping. Binford (1963) notes, however, that these distinguishing features were not exclusive to one category or the other; rather, differentiation was a matter of the frequency of appearance for the respective traits. Recent studies have largely confirmed these findings, with deeper and more prevalent fracturing associated with the burning of fleshed or recently macerated remains (Buikstra and Swegle 1989). These findings also confirm the caveat that differences in fracturing behavior between dry, fleshed, and macerated bone are not mutually exclusive and can only be discussed in terms of degree of presence.

Conditions during and immediately following the burning episode have also been noted to have an influence on the resulting morphological features of

burned bone. For example, rapid cooling of remains after they have been burned will result in a substantial increase in fracturing due to thermal propagation of fractures already present from the burning process (Binford 1963). Differences in the results of burning episodes have also been related to the temperature at which the remains were burned (Quatrehomme et al. 1998). The use of liquid accelerants has also been found to have an effect on the propensity for remains to fracture while burning. In particular, research has shown that use of diesel fuel and turpentine as accelerants results in relatively elevated levels of fragmentation among burned remains (Jackson 2005).

Tests conducted by Bonfield and Li (1965) revealed that the ability of bone to absorb energy before fracturing is severely reduced when it is heated past 200 degrees Celsius. This reduction in the ability to withstand stress should result in microscopic fracture patterns similar to those of fast-propagating fractures when viewed with a scanning electron microscope as reported by Piekarski (Herrmann and Bennett 1999). Microscopic and scanning electron microscopic analysis has also revealed that many of the microstructures present in bone are still visible even after burning. These structures have, however, been shown to undergo alteration in size as a result of burning, although the exact nature of this alteration is still up for debate. Specifically, it appears that osteons and other bone microstructures may ultimately shrink as a result of burning, but it has

been speculated that the process may include a period of expansion before these structures experience a reduction in size (Bradt Miller and Buikstra 1984, Nelson 1992).

Identification of Trauma in Burned Remains

Attempts at identifying trauma in burned remains have largely fallen into one of three categories: studies of heat fracturing in the cranium (Bohnert et al. 1997, Pope and Smith 2004), analysis of sharp force trauma in burned remains (de Gruchy and Rogers 2002, Herrmann and Bennett 1999, Jackson 2005), and differentiation between traumatic and heat fractures (Herrmann and Bennett 1999). The results from early studies of burned crania revealed that heat-induced fractures to this region of the body were believed to be the result of both an increase in the brittleness of the squama and pressure created by the build-up of steam within the crania (Bohnert et al. 1997). More recent research, however, has refuted the steam pressure theory of cranial fracturing (Pope and Smith 2004). Examination of the processes involved in cranial burning exposed the fact that fractures always appear on the convex aspects of the cranium first and typically on the anterior region of the calvarium (Bohnert et al. 1997). The study by Bohnert et al. (1997) also uncovered an absence of heat fracturing to the base of the skull in all observed cases, leading to the conclusion that fractures observed in this region after burning can be reasonably attributed to mechanical trauma.

A study of the morphology of traumatic fractures to the skull after burning conducted by Pope and Smith (2004) revealed several diagnostic features for differentiating between traumatic and burn-related fractures to this area. For instance, they noted that fractures occurring late in the burning process had sharp, well-defined edges, while fractures present before burning tended to have blunt, warped, or otherwise deformed margins resulting from the longer duration of their direct exposure to the fire. Discrepancies in color between adjacent fragments indicated that they were separate for most of the burning process and consequently burned to different degrees. Pope and Smith (2004) also concluded that reconstruction of cranial fragments might reveal convergent or radiating fractures associated with mechanical trauma, and any fractures observed to extend into unburned areas of bone could be attributed to mechanical origins.

Studies of the effects that burning has on sharp force trauma have also distinguished particular characteristics associated with these wounds. For example, de Gruchy and Rogers (2002) found that, while chop marks inflicted on long bones could still be identified after burning, the fire caused a widening of the area in which the blade was extracted. This widening effect was attributed to burning off of the bone fragments that are created when the blade is extracted from the wound. A study conducted by Jackson (2005) using a variety of sharp

instruments revealed that burning can obscure the minute features required for precise identification of the instrument responsible for inflicting the trauma. In particular, he noted that only general categories of “hacking marks” and “knife cuts” could be applied to burned remains with any degree of reliability.

Identification of traumatic fractures in burned remains has arguably been recognized as one of the most difficult undertakings in forensic analysis (Herrmann and Bennett 1999). This is largely due to the high degree of resemblance between these and burn-related fractures. Because of this degree of difficulty, Herrmann and Bennett (1999) recommended a combination of fracture surface morphology and fracture pattern analysis be utilized when attempting to distinguish between traumatic and burn-related fractures.

Microscopic analysis of burned traumatic fractures reveals a somewhat melted appearance on the fracture surface with osteon structures still clearly visible (Herrmann and Bennett 1999). Examination with a scanning electron microscope demonstrates that Haversian pull-outs are still visible along the fracture surface, although these features are less pronounced than in unburned specimens. The rough appearance of these surfaces, often resulting from longitudinal sectioning of Haversian canals, greatly resembles the surfaces of heat fractures making differentiation between the two exceedingly difficult. Fortunately, fractures occurring from mechanical trauma inflicted either late in

the burning episode or subsequent to burning are more easily distinguished. Under microscopic analysis, these fracture surfaces have a smooth appearance, sometimes even exhibiting concentric rings associated with the fracturing of glass-like material.

Implications for Analyzing Blunt Trauma in Burned Ribs

Since it has been determined that burning fleshed bones results in different fracture patterns from dry bones, it would be best to experiment on ribs with flesh still adhering. Doing so would more accurately simulate a forensic scenario in which a perpetrator would burn a body to conceal a crime. Also, because the temperature of the fire has been demonstrated by Bonfield and Li (1965) to affect fracturing, the temperature from each treatment should be closely monitored and kept fairly consistent between treatments. Care should also be taken to insure that the ribs are not completely consumed by the fire, as was the case in the experiment performed by de Gruchy and Rogers (2002). Each treatment should also be allowed to cool naturally so as not to cause further fracturing of the material. The blunt object used to inflict trauma upon the ribs should also remain consistent between treatments and should be something that could reasonably be used as a weapon in a homicide. While these controls may not necessarily reflect the circumstances of every forensic scenario, they are necessary for the accuracy and reproducibility of results.

As Herrmann and Bennett (1999) mentioned, examination of post-burn fractures should include both macroscopic and microscopic analyses due to the difficulty in differentiating fire-related fractures from traumatic fractures. When trying to identify traumatic fracturing, particular attention should be paid to transverse fractures, as these fractures were noted by Galloway (1999) to occur more frequently in cases of direct blunt trauma to the thoracic cage.

Unfortunately, transverse fractures were also found to be more prevalent when burning fleshed bones. Reconstruction of ribs, when possible, may help by establishing how long a fracture was exposed to the fire via analysis of the degree of damage to the fracture edges. Given the amount of bending possible in ribs before reaching failure, evidence of butterfly and greenstick fractures should also be looked for during reconstruction (Galloway 1999). It is possible that the burn damage to greenstick fractures may resemble the damage described by de Gruchy and Rogers (2002) for the blade extraction areas of chop marks, although this is purely speculation.

During microscopic examination, the possible destruction of Haversian pull-outs by burning will make differentiating traumatic fractures from fire-related fractures more difficult since these features were one of the key diagnostics of pre-fire fracturing used by Herrmann and Bennett (1999). Late and post-fire fractures will be easier to distinguish based on their glass-like

appearance. For any microscopic analysis to be possible, however, care will have to be taken in retrieving and storing burned fragments. De Gruchy and Rogers (2002) recommend packing larger fragments in a box with at least 2.5 centimeters of paper towel between each fragment and packing smaller fragments in paper towels before placing them in sealable sandwich bags. They also recommend embedding select fragments in epoxy for thin sectioning for microscopic analysis.

CHAPTER 2

MATERIALS AND METHODS

The use of pig (*Sus scrofa*) remains as a substitute for human cadavers has become a widely accepted practice in forensic studies (Goff 1993). With that in mind, a total of eight racks of spare pork ribs were acquired for use in one of three treatments. Two sets of ribs (Treatments 1 and 2) were placed into a control group that only received blunt force trauma, while two other sets of ribs (Treatments 7 and 8) were placed in a second control group receiving only the burn treatment. The remainder of the ribs (Treatments 3-6) were placed into an experimental treatment group which received blunt force trauma followed by burning.

Blunt force trauma was inflicted with an aluminum baseball bat by placing each rack of ribs on the ground and then striking it a total of five times at an angle parallel to the ribs themselves (Figure 1). This angle of impact would be most logical for an attacker striking a prone victim lying on the ground. Prior to being burned, each set of ribs was x-rayed at the Katy Rehabilitation Hospital to

determine the locations of all traumatic fractures as an aid in fracture identification after the burning event. The racks of ribs used in the burn-only control group were also x-rayed to insure they had not been fractured prior to purchase or during handling. Ribs from the blunt force trauma control group were allowed to decompose naturally from the beginning of September to the end of November in an outdoor location near San Marcos, Texas. This was done so the underlying fractures could be readily observed without the risk of accidental alterations due to maceration. These ribs were protected from potential scavengers (including coyotes and vultures) by a wood-framed, chicken wire cage which was weighted down with rocks and tied to several nearby trees.



Figure 1. Method Used to Inflict Blunt Force Trauma. Photo by Jessica Lyles

Burning of the remainder of the ribs took place in a furnace at Bluebonnet Pet Crematorium (Figure 2). Each set of ribs was pushed into the furnace using a long pole and then slid out onto a cart using the same pole when burning had been completed. Any fragments left in the furnace were scraped into a small chute where they could be collected from a compartment in the bottom of the

furnace and bagged for later reconstruction. Temperature, rate of temperature increase during the burning event, and time in the furnace were carefully recorded during each burning event for purposes of reproducibility (Appendix A). Rate of temperature increase was calculated by noting the furnace temperature at the beginning and end of each burning event, subtracting these two values to determine the total temperature increase, and then dividing this number by the duration of the burning event.



Figure 2. Ribs Being Removed from the Furnace

Before any of the control or experimental ribs were burned, however, an extra set of ribs was placed in the furnace for a total of ten minutes to determine an appropriate burn duration for the rest of the ribs. Given the near total destruction of these ribs, each subsequent set of ribs was allowed to burn for only five minutes; the one exception to this time limit occurred with one of the experimental treatment groups. Treatment 5 was allowed to burn for seven minutes as a way of adding a small element of variation to the burning conditions and to insure that the ribs were receiving the greatest possible burn

damage without being completely destroyed. After the burning was completed, each set of ribs was carefully placed in a box lined with paper towels to prevent damage from occurring during transport. Rib fragments were also wrapped in paper towels before being bagged for transport.

Once all the ribs had been treated, each set was carefully examined with a hand lens in addition to use of the naked eye. Each fracture was given a unique number based on which treatment it came from and on which rib it was found (Appendix B). For example, "Fracture 6.8.1" would be the first fracture on the eighth rib from Treatment 6. Using the previously created x-rays, the initial cause for each observed fracture was noted. Fractures were placed into one of two categories of origin: blunt force trauma or burning event damage. Fractures classified as resulting from the burning event included both heat fractures and fractures caused during extraction from the furnace. No distinction was made between these two causes because of the forensic importance of being able to distinguish blunt force fractures from all other types of fractures. In a few cases, the exact cause of a fracture could not be conclusively determined due to difficulties in matching post-burn fractures with those recorded on the x-ray. Given the uncertain nature of their origin, these fractures were excluded from further analysis. Also, the extended burn time for Treatment 5 made accurate reconstruction of the ribs impossible which led to its exclusion from analysis.

The characteristics used to describe each fracture were pre-selected based on previous studies as well as features the author deemed to be important. Characteristics recorded during visual and hand-lens assessment included appearance of the fracture edge, fracture angle, color of the fracture edge, fracture line, and fracture depth (Appendix C). The first of these characteristics, appearance of the fracture edge, was broken down into one of two possibilities: sharp or dull. Sharp fracture edges included those with a readily apparent, sharply defined margin. Fractures classified as having a dull edge included any fracture whose edge was poorly defined and lacked a sharp, distinct margin.

Fracture angle referred to the angle of the fracture relative to the long axis of the rib on which the fracture occurred and was separated into four categories: longitudinal, transverse, oblique, and curved. Longitudinal fractures were those that occurred along the long axis of the rib. Transverse fractures were those occurring roughly perpendicular to the long axis of the rib, while fractures occurring at approximately a forty-five degree angle to the long axis of the rib were labeled as oblique. Any fracture whose length spanned more than one of these categories was recorded as being curved.

Fracture color specifically refers to the color of the fracture edge at the time of observation after burning. Fracture color was found to be potentially diagnostic in distinguishing between traumatic and burn-related fractures of the

cranium (Pope and Smith 2004). Because the cranium is structurally similar to ribs in that it consists of two thin layers of cortical bone surrounding a layer of trabecular bone, fracture color was included in this analysis. For the sake of consistency in terms of statistical analysis, fracture color was also noted for the treatments that only received blunt force trauma.

The fracture line characteristic was recorded to describe the general path the fracture followed as it propagated. This characteristic was broken into three categories: straight, wavy, and saw-toothed. Fractures classified as straight, as the name implies, included any fracture that followed an essentially straight line across its entire length. Fractures placed in the wavy category included any fractures that appeared to meander as they propagated. The saw-toothed category contained any fracture that exhibited a jagged or splintered fracture line similar to the teeth on a saw blade.

The depth of a fracture was recorded based on how much of the thickness of the rib was separated by the fracture. If, for instance, a fracture only penetrated the cortical bone on the surface of a rib, it was classified as having no depth. A fracture received this classification even if it traversed the entire circumference of the rib, so long as it never penetrated into the underlying trabecular bone. Fractures that succeeded in penetrating into the trabecular bone

of a rib were placed into one of three categories depending on roughly how much of the thickness of the rib was penetrated: 50%, 75%, or 100%.

A series of additional microscopic examinations had also been planned to analyze potential differences in the microscopic structures of burn-related fractures and burned traumatic fractures. Results from a previous study conducted on femora from *Sus scrofa* found slight differences at the microscopic level between these two groups of fractures (Herrmann and Bennett 1999). However, these differences were often very difficult to identify, and this led the authors to conclude that differentiation of fractures based on such characteristics would be tenuous at best. Also, the defining microscopic characteristics separating burn-related fractures from burned traumatic fractures seemed to rely on the persistence of Haversian pull-outs caused by the initial inflicting of blunt force trauma. Unfortunately, given the very small amount of cortical bone present on ribs, it is doubtful that such structures would be present in a traumatic fracture. Furthermore, even if these structures were observable before burning, the fact that the original margins of each traumatic fracture were completely destroyed in all but one or two instances during the burning phase of this experiment makes identification of such pull-out structures impossible. Given these circumstances, it was concluded that microscopic analysis would be a fruitless endeavor and was, therefore, not conducted.

CHAPTER 3

RESULTS

Once all the data for both the control and experimental groups had been compiled, each fracture characteristic was analyzed using chi-squared tests for independence. For the control group, the null hypothesis is that there will be no difference in the distribution of fracture characteristics between the blunt trauma treatment and the burning treatment. The alternate hypothesis for the control group is that there will be a significant difference in the distribution of fracture characteristics between the blunt force and burning treatments. As for the experimental group, the null hypothesis states that there will be no difference in the distribution of fracture characteristics between fractures resulting from the burning event and fractures initially created by blunt force trauma prior to burning. The alternate hypothesis for this group is that a significant difference in the distribution of fracture characteristics will exist between fractures caused by the burning event and blunt force fractures that were subsequently burned. In all cases, a critical value of .05 will be used to determine significance.

Control Group

Analysis of fracture color was conducted for the control group first.

Although there is no question as to the significance of fracture cause on fracture color for the control group, statistical analysis was still carried out to insure that the analytical tools being used were accurately measuring the desired relationships. Examination of the frequencies observed for each color compared to the expected frequencies if no relationship existed between fracture cause and fracture color revealed that virtually all of the blunt force fractures were brown in color (Table 1). Burn fractures, on the other hand, were distributed among the black, grey, and white categories with over half falling into the black category.

Table 1. Frequency Table for Fracture Color in the Control Group

			Color				Total
			Black	Grey	White	Brown	
Cause	Blunt	Count	0	0	0	16	16
		Expected Count	7.7	2.6	3.5	2.2	16.0
	Burn Event	Count	57	19	26	0	102
		Expected Count	49.3	16.4	22.5	13.8	102.0
Total		Count	57	19	26	16	118
		Expected Count	57.0	19.0	26.0	16.0	118.0

Analyses of these data produce a chi-square value of 118.000 which, at three degrees of freedom, results in a two-tailed significance value of .000.

Normally, this significance value might be called into question by the fact that three of the cells in Table 1 have expected counts of less than five. The presence

of an expected value less than five for any category can artificially inflate the chi-square value for that analysis. However, given the complete separation of blunt force fractures and burn fractures into discrete color categories, which can be demonstrated by a Cramer's V value of 1.000 for this chi-square test, it seems more than reasonable to accept the validity of the test. Therefore, the null hypothesis can be rejected for fracture color in the control group.

Assessment of observed and expected frequencies for fracture angle in the control group shows double the number of transverse blunt force fractures expected (Table 2). Longitudinal fractures, on the other hand, are more prevalent in the burn treatments, making up exactly half of the observed fractures from the burn group. Statistical analysis for fracture angle produces a chi-square value of 13.722; at three degrees of freedom, this equates to a two-tailed significance value of .003. Unfortunately, the expected frequencies for oblique and curved blunt force fractures are less than five. Since there is only a .2 difference between observed and expected values for oblique and curved fractures, fractures falling into these categories were simply excluded from the analysis which eliminated a total of 28 fractures. Reevaluation of the data based solely on the distribution of longitudinal and transverse fractures produces a chi-square value of 13.876 which has a two-tailed significance of .000 with one degree of freedom. This means the null hypothesis can also be rejected for fracture angle. In addition, the

Cramer's V value for this test came out to .393, indicating that fracture cause seems to have a moderate effect on fracture angle (Gravetter and Wallnau 2007).

Table 2. Frequency Table for Fracture Angle in the Control Group

			Angle				Total
			Longitudinal	Transverse	Oblique	Curved	
Cause	Blunt	Count	1	11	2	2	16
		Expected Count	7.1	5.2	1.8	2.0	16.0
	Burn Event	Count	51	27	11	13	102
		Expected Count	44.9	32.8	11.2	13.0	102.0
Total		Count	52	38	13	15	118
		Expected Count	52.0	38.0	13.0	15.0	118.0

Observed and expected frequencies for fracture line reveal a greater tendency for burn fractures to be straight, while blunt force fractures are less likely to be straight than would otherwise be expected (Table 3). However, the opposite seems to be true concerning saw-like fractures. Statistical assessment of the data generates a chi-square value of 7.351 with two degrees of freedom which produces a two-tailed significance value of .025. Once again, this value is called into question by the low expected counts for wavy and saw-like blunt force fractures. Since the greatest differences between observed and expected frequencies have occurred for straight fractures, this problem was overcome by combining the other two categories into a single category labeled "Other" (Table 4). Reassessment of the data reveals a chi-square value of 4.575 which, with only one degree of freedom, produces a two-tailed significance of .032. While this

value is good enough to reject the null hypothesis, the Cramer's V value of .197 indicates that fracture cause has only a small effect on fracture line (Gravetter and Wallnau 2007).

Table 3. Frequency Table for Fracture Line in the Control Group

			Line			Total
			Straight	Wavy	Saw	
Cause	Blunt	Count	5	5	6	16
		Expected Count	8.9	4.5	2.6	16.0
	Burn Event	Count	61	28	13	102
		Expected Count	57.1	28.5	16.4	102.0
Total		Count	66	33	19	118
		Expected Count	66.0	33.0	19.0	118.0

Table 4. Condensed Frequency Table for Fracture Line in the Control Group

			Line		Total
			Straight	Other	
Cause	Blunt	Count	5	11	16
		Expected Count	8.9	7.1	16.0
	Burn Event	Count	61	41	102
		Expected Count	57.1	44.9	102.0
Total		Count	66	52	118
		Expected Count	66.0	52.0	118.0

Examination of fracture edge reveals a definite tendency for blunt force fractures to have a dull edge while burn fractures are more likely to have sharp edges (Table 5). Analysis of the data at one degree of freedom produces a chi-square value of 18.522 with a two-tailed significance of .000. This value easily surpasses the .05 critical value necessary for rejecting the null hypothesis.

Furthermore, the Cramer's V value of .396 indicates that fracture cause has a moderate effect on fracture edge (Gravetter and Wallnau 2007).

Table 5. Frequency Table for Fracture Edge in the Control Group

			Edge		Total
			Sharp	Dull	
Cause	Blunt	Count	3	13	16
		Expected Count	10.6	5.4	16.0
	Burn Event	Count	75	27	102
		Expected Count	67.4	34.6	102.0
Total		Count	78	40	118
		Expected Count	78.0	40.0	118.0

Assessment of observed and expected frequencies for fracture depth demonstrates a distinct tendency for blunt force fractures to have a depth of 50% or more (Table 6). On the other hand, only the frequency of burn fractures with no appreciable depth is higher than expected. This clear distinction between blunt force and burn fractures results in a chi-square value of 30.080 which has a two-tailed significance of .000 with three degrees of freedom. However, due to low expected frequencies, the three greatest depth categories had to be combined to achieve statistically reliable results. This subsequent comparison of fractures having no appreciable depth with those having some depth (Table 7) produces a chi-square value of 23.341 which, at only one degree of freedom, still allows the null hypothesis to be rejected with a two-tailed significance of .000. With a

Cramer's V value of .445, fracture cause also seems to have a moderate effect on fracture depth (Gravetter and Wallnau 2007).

Table 6. Frequency Table for Fracture Depth in the Control Group

			Depth				Total
			None	50%	75%	100%	
Cause	Blunt	Count	1	3	3	9	16
		Expected Count	9.8	1.4	.5	4.3	16.0
	Burn Event	Count	71	7	1	23	102
		Expected Count	62.2	8.6	3.5	27.7	102.0
Total		Count	72	10	4	32	118
		Expected Count	72.0	10.0	4.0	32.0	118.0

Table 7. Condensed Frequency Table for Fracture Depth in the Control Group

			Depth		Total
			None	Some	
Cause	Blunt	Count	1	15	16
		Expected Count	9.8	6.2	16.0
	Burn event	Count	71	31	102
		Expected Count	62.2	39.8	102.0
Total		Count	72	46	118
		Expected Count	72.0	46.0	118.0

Experimental Group

Analysis of fracture color for the experimental group reveals observed frequencies for each color that are very close to those values expected if there was no relationship between fracture cause and fracture color (Table 8). The brown category was added to the fracture color variable for the experimental data because one blunt force trauma fracture failed to burn at all, thereby

retaining a brownish coloring similar to fractures from the blunt force control group. The chi-square value for fracture color is 3.541 which, at three degrees of freedom, equates to a two-tailed significance value of .315. This significance value fails to meet the .05 critical value used for this study which means the null hypothesis can not be rejected for fracture color.

Table 8. Frequency Table for Fracture Color in the Experimental Group

			Color				Total
			Black	Grey	White	Brown	
Cause	Blunt	Count	20	2	3	1	26
		Expected Count	20.8	2.3	2.7	.2	26.0
	Burn Event	Count	72	8	9	0	89
		Expected Count	71.2	7.7	9.3	.8	89.0
Total		Count	92	10	12	1	115
		Expected Count	92.0	10.0	12.0	1.0	115.0

Examination of observed and expected frequencies for fracture angle in the experimental group reveals that less than half the expected number of longitudinal fractures are actually observed for the blunt force fracture group, while transverse fractures for this group are twice what was expected (Table 9). Frequencies for the burn-related fractures, on the other hand, are higher than expected for longitudinal fractures and lower than expected for transverse fractures. The chi-square value for fracture angle came out to 19.396; at three degrees of freedom, this results in a two-tailed significance value of .000.

Table 9. Frequency Table for Fracture Angle in the Experimental Group

			Angle				Total
			Longitudinal	Transverse	Oblique	Curved	
Cause	Blunt	Count	5	14	4	3	26
		Expected Count	12.9	6.3	2.7	4.1	26.0
	Burn Event	Count	52	14	8	15	89
		Expected Count	44.1	21.7	9.3	13.9	89.0
Total	Count		57	28	12	18	115
	Expected Count		57.0	28.0	12.0	18.0	115.0

While this value would be more than enough to reject the null hypothesis, the fact that two of the expected values for fracture angle in the blunt force category are less than five (2.7 for oblique and 4.1 for curved) cast doubt on the results. Consequently, a second analysis was conducted with all curved and oblique fractures being combined into a single category labeled "Other" (Table 10). This corrected the problem and returned a chi-square value of 18.252 which, with only two degrees of freedom, still produces a significance value of .000. The null hypothesis can now safely be rejected for fracture angle. Furthermore, the Cramer's V value for this analysis was .398. This means that not only is there a significant difference in fracture angle between blunt force fractures and burn-related fractures, but that fracture cause has a moderate effect on fracture angle (Gravetter and Wallnau 2007).

Table 10. Condensed Frequency Table for Fracture Angle in the Experimental Group

			Angle			Total
			Longitudinal	Transverse	Other	
Cause	Blunt	Count	5	14	7	26
		Expected Count	12.9	6.3	6.8	26.0
	Burn Event	Count	52	14	23	89
		Expected Count	44.1	21.7	23.2	89.0
Total		Count	57	28	30	115
		Expected Count	57.0	28.0	30.0	115.0

Examination of observed frequencies for the fracture line characteristic among traumatic fractures finds them to be slightly less than expected for straight fractures and twice that expected for saw-like fractures (Table 11). On the other hand, there are slightly more straight fractures and fewer saw-like fractures than expected for the burn event category. These differences generate a chi-square value of 8.428 which is significant with a two-tailed value of .015 and two degrees of freedom; this means the null hypothesis can be rejected for the fracture line characteristic. However, with a Cramer's V value of .271, it seems that fracture cause has only a small effect on fracture line (Gravetter and Wallnau 2007).

Table 11. Frequency Table for Fracture Line in the Experimental Group

			Line			Total
			Straight	Wavy	Saw	
Cause	Blunt	Count	8	8	10	26
		Expected Count	12.0	9.0	5.0	26.0
	Burn Event	Count	45	32	12	89
		Expected Count	41.0	31.0	17.0	89.0
Total		Count	53	40	22	115
		Expected Count	53.0	40.0	22.0	115.0

The difference between observed and expected frequencies is only two for each category in the examination of the fracture edge characteristic (Table 12). The chi-square value for this analysis is 1.279 which, with one degree of freedom, produces a two-tailed significance value of .258. Not surprisingly, given the uniformity of the observed and expected frequencies, this value fails to reject the null hypothesis for the fracture line characteristic.

Table 12. Frequency Table for Fracture Edge in the Experimental Group

			Edge		Total
			Sharp	Dull	
Cause	Blunt	Count	18	8	26
		Expected Count	20.1	5.9	26.0
	Burn Event	Count	71	18	89
		Expected Count	68.9	20.1	89.0
Total		Count	89	26	115
		Expected Count	89.0	26.0	115.0

Examination of frequencies for the depth characteristic reveal fewer fractures with no depth than expected for the blunt force category and more

fractures with this characteristic than expected for the burn event category (Table 13). The opposite of this trend is true for every other fracture depth with blunt force fractures having higher frequencies than expected while burn-related fractures have frequencies that are lower than expected. With three degrees of freedom, the resulting chi-square value of 47.134 achieves a two-tailed significance of .000. Once again, however, expected frequencies for the 50% and 75% depth categories are less than five. Simply combining these two categories proved insufficient to correct the problem, so all the fractures were compiled into just two categories: those having no depth and those having some depth (Table 14). Reanalyzing the data produces the same significance value as before, only this time with a chi-square value of 44.523 and one degree of freedom, meaning the null hypothesis can be securely rejected. Additionally, with a Cramer's V value of .622, fracture cause appears to have a fairly large effect on fracture depth (Gravetter and Wallnau 2007).

Table 13. Frequency Table for Fracture Depth in the Experimental Group

			Depth				Total
			None	50%	75%	100%	
Cause	Blunt	Count	5	5	1	15	26
		Expected Count	18.5	1.4	.2	5.9	26.0
	Burn Event	Count	77	1	0	11	89
		Expected Count	63.5	4.6	.8	20.1	89.0
Total	Count		82	6	1	26	115
	Expected Count		82.0	6.0	1.0	26.0	115.0

Table 14. Condensed Frequency Table for Fracture Depth in the Experimental Group

			Depth		Total
			None	Some	
Cause	Blunt	Count	5	21	26
		Expected Count	18.5	7.5	26.0
	Burn Event	Count	77	12	89
		Expected Count	63.5	25.5	89.0
Total	Count		82	33	115
	Expected Count		82.0	33.0	115.0

CHAPTER 4

DISCUSSION

Statistical analysis of the control material reveals that all five fracture characteristics have a significant relationship to fracture cause, the most obvious of which is color. Blunt force fractures exhibit a brownish color resulting from being allowed to decompose naturally in an outdoor setting, while burn fractures vary along a continuum from black to white. In terms of fracture angle, blunt force is most likely to produce transverse fracturing of the ribs; this finding is consistent with information reported by Galloway (1999). However, burn fractures are found to be predominantly longitudinal, a discovery that contradicts previous studies of long bones (Binford 1963, Buikstra and Swegle 1989, Herrmann and Bennett 1999). Burn conditions are also more likely to produce straight fractures and fractures with sharp edges, while blunt force fractures tend to have a dull edge and typically lack a straight line of propagation. Both of these characteristics seem to be consistent with the notion that fractures occurring in burned bone should resemble rapidly propagating

fractures (Herrmann and Bennett 1999). Finally, all but one of the blunt force fractures have a depth of at least 50%, while approximately two-thirds of the burn fractures lack any appreciable depth.

However, not all of these fracture characteristics maintain a significant relationship to fracture cause when applied to the experimental group. For instance, fracture color fails to show a significant relationship to fracture cause in the experimental group with the majority of all fractures having a black edge. This finding differed from the results reported by Pope and Smith (2004) in their study of traumatic fractures in burned crania, in which black fracture edges were indicative of trauma present before burning. Fracture edge also fails to achieve significance for the experimental group, possibly due to the destruction of the initial fracture surface on many of the blunt force fractures during burning.

Of the fracture characteristics that remain significant for the experimental group, fracture depth might well be the best indicator of fracture cause. Not only does it have a very low significance value, but Cramer's V indicates that fracture cause has a great deal of influence on depth. This means that fractures lacking any appreciable depth are more likely to be caused by the burn event, while deep or complete fractures are more likely to be indicative of blunt force trauma.

Fracture angle also appears to be a decent indicator of fracture cause. This characteristic has a significance value as impressive as fracture depth and, based

on Cramer's V , a fracture's cause has a moderate influence on its angle. Consequently, transverse fractures seem to be indicative of blunt force trauma as reported by Galloway (1999). However, unlike findings reported by Binford (1963), Buikstra and Swegle (1989), and Herrmann and Bennett (1999), longitudinal fractures were found to be more common among burn-related fractures.

While fracture line also remains significantly related to fracture cause in the experimental group, its usefulness as an indicator of fracture cause is somewhat questionable. For one thing, its significance value, while still well below the .05 critical value set for this experiment, is not as impressive as those for fracture angle and depth. Also, the Cramer's V value indicates that fracture cause has only a small influence on fracture line, meaning these characteristics should be viewed with caution. Still, the results show that blunt force fractures tend toward saw-like fracture lines. Also, contrary to the findings of Thurman and Wilmore (1981), fractures resulting from the burn event seem more likely to exhibit a straight fracture line.

In addition to the reported statistical findings, a few general observations were also made concerning the experimental material. While these observations may not be quantifiable in any meaningful sense, they are nevertheless intriguing enough to warrant mention. The first such observation concerns the

blunt force fracture from Treatment 6 that failed to burn while in the furnace. This fracture possesses similar characteristics to fractures from the blunt force control group and is, in particular, the only fracture from the entire experimental group that has a brownish color. While it might seem obvious to say that fractures bearing this coloration are doubtlessly not the result of burning, it does not mean that their presence among burned remains indicates they occurred prior to burning. If a portion of a rib remains unburned, it can still be subsequently fractured by some mechanical means. In this case, the question becomes a matter of determining whether the fracture was a fresh or dry-bone break.

Another observation during analysis of the experimental material concerns burn patterns around pre-existing defects in several of the ribs. In this case, the term “pre-existing defect” refers not only to blunt force fractures inflicted before burning, but also to the sharp force trauma left on the ends of the ribs by the butcher. In several instances, these defects exhibit greater destruction of the adjacent cortical bone relative to that of the trabecular bone. This results in exposed areas of trabecular bone near the margins of these defects (Figure 3). A couple of explanations may exist for this phenomenon. It is possible that exposing the cross-sectional area of the bone makes it more susceptible to delamination while burning. However, it is equally possible that being adjacent

to such a defect makes the cortical bone more fragile and prone to flaking off during subsequent handling.



Figure 3. Exposure of Trabecular Bone Around a Transverse Blunt Force Fracture

One final observation involves two of the blows inflicted with the blunt instrument; both of these blows resulted in crushing fractures of the ribs they struck. In both instances, the damage resulted in splintering and fragmentation of the rib instead of a clean break. When these ribs were subsequently burned, the splintered ends of the fractures curled up and away from the fractures' margins (Figure 4). This phenomenon was not observed in any other fractures, traumatic or burn-related, but has been reported to occur when cremating fleshed bone (Binford 1963, Thurman and Wilmore 1981). Owing to the similarity between the splintered edges of these fractures and those found in greenstick fractures, not to mention the unfortunate lack of greenstick fractures

in the present study, it would be interesting to see if greenstick fractures also exhibit this characteristic when burned.



Figure 4. Warped Splinter of Bone from a Crushing Fracture

The absence of greenstick fractures calls attention to one of the errors of methodology in this study. By simply placing the ribs on a hard surface and subsequently striking them with a blunt instrument, the ribs were denied the freedom to bend far enough to achieve a greenstick fracture. This problem could have been avoided by using whole carcasses instead of merely racks of ribs. However, even if whole carcasses had been used, there is some question as to whether the difference in curvature between *Sus scrofa* ribs and human ribs might interfere with the ability to generalize between the two. This dilemma comes from the effect rib curvature has on the location and angle of fractures (Galloway 1999).

Another obvious problem with the present study is the relatively small number of blunt fractures. In the case of the blunt force control treatments, this

problem could have been remedied by simply striking each set of ribs more times. While this could have also been done for the experimental treatments, concerns begin to arise involving the ability to accurately reconstruct the ribs after they have been burned. Therefore, the number of blunt force fractures could have been safely increased by adding more treatments to the control group. While this would have little effect on the ratio of blunt force fractures to burn fractures, it would have most likely eliminated the problems with low expected frequencies during statistical analysis.

Finally, it should be noted that the findings from this study, given the very controlled nature under which it was conducted, are really only applicable to situations where burned remains are left relatively undisturbed, both during and after the burning process. Anything more than a minor disturbance of such remains, whether intentional or not, would likely invalidate many of the results from the present study. The potential for a loss of evidence through handling provides support for the importance of having a forensic anthropologist present at the scene of a body recovery. At any rate, before these results could be properly applied to a legitimate forensic scenario, blind tests of the findings from this study would have to be conducted to see if fracture line, fracture angle, or fracture depth are significant indicators of fracture cause. Even then, a body can be burned under a variety of different conditions including variations in

temperature, burn time, and use of accelerants to name a few. Each of these variables would also have to be investigated, leaving room for a great deal of further research for which this study can hopefully provide a solid base.

APPENDIX A

TIME AND TEMPERATURE DATA FOR BURN EVENTS

Table 15. Burn Conditions for Each Treatment

Treatment	Burn Time (min.)	Starting Temp. (°C)	Ending Temp. (°C)	Rate of Temp. Increase (C°/min.)
Test Run	10	593	699	10.6
3	5	608	688	16.0
4	5	638	692	10.8
5	7	650	743	13.3
6	5	678	762	16.8
7	5	653	715	12.4
8	5	714	779	13.0

APPENDIX B

RAW DATA

Table 16. Complete Listing of Information for Each Fracture

Fracture	Cause	Color	Angle	Line	Edge	Depth
1.6.1	blunt force	brown	longitudinal	straight	sharp	100%
1.6.2	blunt force	brown	transverse	saw	dull	100%
1.6.3	blunt force	brown	oblique	wavy	dull	100%
1.7.1	blunt force	brown	transverse	wavy	sharp	75%
1.8.1	blunt force	brown	transverse	saw	dull	100%
1.9.1	blunt force	brown	curved	straight	dull	50%
1.9.2	blunt force	brown	transverse	saw	dull	100%
1.9.3	blunt force	brown	transverse	wavy	dull	none
1.10.1	blunt force	brown	transverse	straight	dull	100%
1.10.2	blunt force	brown	curved	straight	dull	50%
2.2.1	blunt force	brown	transverse	saw	dull	75%
2.3.1	blunt force	brown	transverse	saw	dull	100%
2.4.1	blunt force	brown	transverse	saw	dull	75%
2.6.1	blunt force	brown	transverse	wavy	dull	100%
2.7.1	blunt force	brown	transverse	straight	dull	50%
2.9.1	blunt force	brown	oblique	wavy	sharp	100%
3.3.1	burn event	black	transverse	straight	sharp	50%
3.3.2	burn event	black	longitudinal	straight	dull	100%
3.3.3	burn event	black	longitudinal	wavy	dull	none
3.3.4	burn event	white	curved	straight	sharp	none
3.3.5	burn event	white	longitudinal	straight	sharp	none
3.4.1	burn event	black	longitudinal	wavy	sharp	none
3.4.2	burn event	black	oblique	wavy	sharp	none
3.4.3	burn event	black	transverse	wavy	sharp	none

Table 16-Continued

Fracture	Cause	Color	Angle	Line	Edge	Depth
3.4.4	burn event	grey	curved	straight	sharp	none
3.4.5	burn event	black	longitudinal	wavy	sharp	none
3.4.6	blunt force	black	transverse	straight	dull	50%
3.4.7	blunt force	black	oblique	straight	sharp	100%
3.4.8	blunt force	black	oblique	saw	sharp	100%
3.4.9	burn event	black	longitudinal	straight	dull	none
3.4.10	burn event	black	curved	wavy	dull	none
3.6.1	burn event	black	longitudinal	straight	sharp	none
3.6.2	blunt force	black	transverse	wavy	dull	50%
3.6.3	blunt force	black	longitudinal	wavy	sharp	100%
3.7.1	burn event	black	transverse	wavy	sharp	none
3.7.2	blunt force	black	transverse	wavy	sharp	none
3.7.3	burn event	black	longitudinal	wavy	dull	none
3.7.4	burn event	black	longitudinal	straight	sharp	none
3.8.1	burn event	black	longitudinal	straight	sharp	none
3.8.2	blunt force	grey	transverse	saw	sharp	75%
3.8.3	burn event	black	longitudinal	straight	sharp	none
3.8.4	burn event	black	longitudinal	straight	dull	none
3.8.5	blunt force	black	transverse	saw	dull	none
3.9.1	burn event	black	longitudinal	wavy	sharp	none
3.9.2	burn event	black	transverse	straight	sharp	none
3.9.3	burn event	black	longitudinal	wavy	sharp	none
3.9.4	burn event	grey	transverse	straight	sharp	none
3.9.5	burn event	black	oblique	wavy	dull	none
3.9.6	blunt force	black	transverse	saw	sharp	50%
3.9.7	burn event	grey	longitudinal	wavy	sharp	none
3.10.1	blunt force	black	transverse	saw	sharp	100%
3.10.2	burn event	black	longitudinal	straight	sharp	none
3.10.3	burn event	black	longitudinal	saw	sharp	none
3.10.4	burn event	black	curved	straight	dull	none
3.11.1	burn event	black	longitudinal	straight	sharp	none
3.11.2	burn event	black	curved	straight	sharp	none

Table 16-Continued

Fracture	Cause	Color	Angle	Line	Edge	Depth
3.11.3	burn event	black	oblique	wavy	sharp	none
4.2.1	burn event	black	oblique	saw	dull	none
4.3.1	burn event	black	curved	wavy	sharp	none
4.3.2	burn event	black	curved	wavy	sharp	none
4.4.1	blunt force	black	oblique	wavy	sharp	100%
4.4.2	burn event	black	curved	straight	sharp	none
4.4.3	burn event	black	longitudinal	wavy	sharp	100%
4.5.1	burn event	black	oblique	straight	sharp	100%
4.5.2	burn event	black	longitudinal	saw	sharp	none
4.5.3	burn event	black	longitudinal	wavy	sharp	none
4.5.4	burn event	grey	longitudinal	wavy	sharp	none
4.6.1	blunt force	black	curved	straight	sharp	none
4.6.2	blunt force	black	transverse	saw	sharp	100%
4.6.3	burn event	white	longitudinal	straight	sharp	none
4.6.4	burn event	grey	longitudinal	straight	sharp	none
4.7.1	burn event	black	longitudinal	straight	sharp	none
4.7.2	burn event	black	transverse	straight	sharp	none
4.7.3	blunt force	black	transverse	saw	sharp	100%
4.7.4	blunt force	black	longitudinal	straight	sharp	100%
4.7.5	blunt force	black	longitudinal	straight	sharp	100%
4.7.6	blunt force	white	longitudinal	straight	sharp	100%
4.8.1	burn event	black	curved	straight	sharp	none
4.8.2	burn event	black	longitudinal	straight	sharp	none
4.8.3	burn event	black	transverse	straight	sharp	none
4.8.4	burn event	black	longitudinal	wavy	sharp	none
4.9.1	burn event	black	longitudinal	wavy	sharp	none
4.9.2	burn event	black	curved	straight	dull	none
4.9.3	burn event	grey	transverse	saw	dull	none
4.9.4	burn event	grey	transverse	straight	sharp	none
4.9.5	blunt force	black	curved	straight	dull	none
4.9.6	blunt force	black	curved	saw	dull	none
4.10.1	blunt force	white	transverse	saw	sharp	100%

Table 16-Continued

Fracture	Cause	Color	Angle	Line	Edge	Depth
4.10.2	blunt force	white	transverse	saw	dull	100%
4.10.3	burn event	black	longitudinal	straight	sharp	none
4.10.4	burn event	white	longitudinal	straight	sharp	none
4.10.5	burn event	white	longitudinal	straight	sharp	none
4.11.1	burn event	black	transverse	saw	sharp	100%
4.11.2	burn event	white	longitudinal	straight	sharp	none
4.11.3	burn event	black	oblique	saw	sharp	none
4.11.4	burn event	black	longitudinal	straight	sharp	none
4.11.5	burn event	black	longitudinal	straight	sharp	none
6.4.1	burn event	black	curved	saw	dull	none
6.5.1	burn event	black	longitudinal	straight	sharp	none
6.5.2	burn event	grey	transverse	wavy	sharp	none
6.5.3	burn event	black	longitudinal	straight	dull	none
6.6.1	burn event	black	longitudinal	wavy	sharp	100%
6.6.2	burn event	black	longitudinal	wavy	sharp	none
6.6.3	burn event	black	transverse	wavy	dull	100%
6.7.1	blunt force	black	oblique	wavy	sharp	100%
6.7.2	burn event	black	longitudinal	straight	sharp	none
6.7.3	burn event	black	longitudinal	straight	sharp	none
6.7.4	burn event	black	curved	saw	sharp	none
6.8.1	burn event	black	curved	straight	sharp	none
6.8.2	burn event	black	longitudinal	straight	sharp	none
6.8.3	burn event	black	oblique	wavy	dull	100%
6.8.4	burn event	black	oblique	saw	sharp	none
6.8.5	burn event	black	longitudinal	straight	sharp	100%
6.9.1	blunt force	brown	transverse	straight	dull	100%
6.9.2	burn event	black	longitudinal	straight	sharp	100%
6.9.3	burn event	black	longitudinal	saw	sharp	none
6.9.4	burn event	black	transverse	saw	sharp	100%
6.9.5	burn event	white	longitudinal	straight	sharp	none
6.9.6	burn event	white	longitudinal	wavy	dull	none
6.9.7	burn event	white	longitudinal	wavy	dull	none

Table 16-Continued

Fracture	Cause	Color	Angle	Line	Edge	Depth
6.10.1	blunt force	black	transverse	wavy	dull	50%
6.10.2	burn event	black	longitudinal	straight	sharp	none
6.10.3	blunt force	grey	longitudinal	wavy	sharp	50%
6.10.4	burn event	black	longitudinal	wavy	sharp	none
6.10.5	burn event	black	longitudinal	wavy	sharp	none
6.10.6	burn event	black	transverse	saw	sharp	100%
6.11.1	blunt force	black	transverse	wavy	sharp	100%
6.11.2	burn event	black	longitudinal	straight	sharp	none
6.11.3	burn event	black	longitudinal	wavy	sharp	none
6.11.4	burn event	black	curved	wavy	sharp	none
6.11.5	burn event	black	curved	wavy	dull	none
7.1.1	burn event	black	longitudinal	straight	dull	50%
7.2.1	burn event	black	curved	straight	dull	50%
7.2.2	burn event	black	curved	straight	sharp	none
7.2.3	burn event	black	transverse	saw	sharp	100%
7.4.1	burn event	black	longitudinal	straight	sharp	50%
7.4.2	burn event	white	transverse	straight	sharp	none
7.4.3	burn event	grey	transverse	saw	sharp	50%
7.4.4	burn event	grey	transverse	straight	sharp	none
7.4.5	burn event	black	longitudinal	straight	sharp	50%
7.4.6	burn event	black	longitudinal	wavy	sharp	none
7.4.7	burn event	black	longitudinal	straight	dull	none
7.5.1	burn event	black	longitudinal	straight	sharp	100%
7.5.2	burn event	black	transverse	straight	sharp	none
7.5.3	burn event	black	transverse	saw	sharp	100%
7.5.4	burn event	black	longitudinal	wavy	sharp	none
7.5.5	burn event	black	transverse	straight	sharp	none
7.6.1	burn event	white	longitudinal	wavy	sharp	100%
7.6.2	burn event	black	transverse	straight	sharp	none
7.6.3	burn event	white	longitudinal	straight	sharp	50%
7.6.4	burn event	white	curved	straight	sharp	none
7.6.5	burn event	white	oblique	straight	sharp	none

Table 16-Continued

Fracture	Cause	Color	Angle	Line	Edge	Depth
7.6.6	burn event	black	transverse	straight	dull	100%
7.7.1	burn event	black	longitudinal	straight	sharp	100%
7.7.2	burn event	white	longitudinal	straight	sharp	none
7.7.3	burn event	white	oblique	saw	sharp	100%
7.7.4	burn event	black	longitudinal	straight	sharp	none
7.7.5	burn event	black	longitudinal	straight	sharp	none
7.8.1	burn event	black	longitudinal	straight	dull	100%
7.8.2	burn event	black	longitudinal	straight	sharp	none
7.8.3	burn event	black	transverse	saw	dull	100%
7.8.4	burn event	white	transverse	straight	sharp	none
7.8.5	burn event	white	curved	straight	sharp	none
7.9.1	burn event	black	longitudinal	straight	sharp	100%
7.9.2	burn event	black	oblique	saw	sharp	none
7.9.3	burn event	black	longitudinal	wavy	sharp	none
7.9.4	burn event	black	curved	straight	sharp	none
7.9.5	burn event	black	transverse	wavy	sharp	100%
7.10.1	burn event	black	transverse	wavy	sharp	100%
7.10.2	burn event	black	longitudinal	straight	sharp	none
7.10.3	burn event	black	longitudinal	wavy	dull	none
7.10.4	burn event	black	curved	wavy	dull	none
7.11.1	burn event	black	transverse	saw	sharp	100%
7.11.2	burn event	black	longitudinal	wavy	sharp	none
7.11.3	burn event	black	longitudinal	straight	sharp	none
8.1.1	burn event	black	longitudinal	straight	sharp	none
8.1.2	burn event	grey	longitudinal	wavy	sharp	75%
8.1.3	burn event	grey	transverse	wavy	dull	none
8.1.4	burn event	grey	transverse	wavy	sharp	none
8.2.1	burn event	black	longitudinal	straight	dull	100%
8.2.2	burn event	black	longitudinal	straight	sharp	none
8.3.1	burn event	white	longitudinal	straight	sharp	100%
8.3.2	burn event	black	longitudinal	straight	sharp	none
8.4.1	burn event	grey	longitudinal	straight	sharp	none

Table 16-Continued

Fracture	Cause	Color	Angle	Line	Edge	Depth
8.4.2	burn event	white	longitudinal	straight	dull	none
8.4.3	burn event	black	longitudinal	straight	dull	100%
8.5.1	burn event	black	longitudinal	straight	sharp	100%
8.5.2	burn event	grey	curved	wavy	sharp	none
8.6.1	burn event	grey	transverse	straight	sharp	none
8.6.2	burn event	white	oblique	wavy	dull	none
8.6.3	burn event	grey	curved	wavy	sharp	none
8.6.4	burn event	black	longitudinal	straight	sharp	100%
8.7.1	burn event	black	longitudinal	wavy	sharp	100%
8.7.2	burn event	black	transverse	straight	sharp	none
8.7.3	burn event	black	transverse	straight	sharp	none
8.7.4	burn event	black	transverse	straight	sharp	none
8.7.5	burn event	black	oblique	straight	sharp	none
8.7.6	burn event	black	curved	straight	sharp	none
8.7.7	burn event	white	transverse	wavy	sharp	none
8.7.8	burn event	grey	oblique	wavy	dull	none
8.8.1	burn event	black	transverse	wavy	sharp	100%
8.8.2	burn event	black	longitudinal	straight	sharp	none
8.8.3	burn event	black	longitudinal	wavy	dull	none
8.8.4	burn event	black	transverse	straight	sharp	none
8.8.5	burn event	black	oblique	saw	sharp	none
8.9.1	burn event	white	longitudinal	straight	sharp	none
8.9.2	burn event	white	oblique	straight	sharp	none
8.9.3	burn event	grey	transverse	straight	dull	none
8.9.4	burn event	black	longitudinal	wavy	sharp	none
8.9.5	burn event	grey	oblique	straight	dull	none
8.9.6	burn event	black	longitudinal	straight	dull	none
8.9.7	burn event	grey	curved	saw	dull	none
8.9.8	burn event	black	longitudinal	straight	sharp	none
8.9.9	burn event	black	longitudinal	straight	sharp	none
8.10.1	burn event	black	longitudinal	straight	sharp	100%
8.10.2	burn event	white	transverse	straight	sharp	none

Table 16-Continued

Fracture	Cause	Color	Angle	Line	Edge	Depth
8.10.3	burn event	grey	transverse	straight	sharp	none
8.10.4	burn event	white	transverse	saw	sharp	none
8.10.5	burn event	grey	longitudinal	wavy	dull	none
8.10.6	burn event	grey	longitudinal	wavy	dull	none
8.10.7	burn event	grey	curved	wavy	dull	none
8.10.8	burn event	black	longitudinal	wavy	dull	none
8.11.1	burn event	white	longitudinal	straight	dull	none
8.11.2	burn event	white	curved	straight	sharp	none
8.11.3	burn event	white	longitudinal	straight	sharp	50%
8.11.4	burn event	white	longitudinal	straight	sharp	none
8.11.5	burn event	grey	longitudinal	straight	sharp	100%
8.11.6	burn event	white	oblique	saw	sharp	100%
8.11.7	burn event	white	longitudinal	wavy	dull	none
8.11.8	burn event	white	longitudinal	wavy	sharp	none
8.11.9	burn event	white	longitudinal	wavy	dull	none
8.11.10	burn event	white	curved	saw	sharp	none
8.11.11	burn event	grey	oblique	saw	dull	none

APPENDIX C

VISUAL ATLAS OF FRACTURE CHARACTERISTICS

Fracture Color



Figure 5. A Black Fracture



Figure 6. A White Fracture



Figure 7. A Grey Fracture



Figure 8. A Brown Fracture

Fracture Angle



Figure 9. A Longitudinal Fracture



Figure 10. A Transverse Fracture

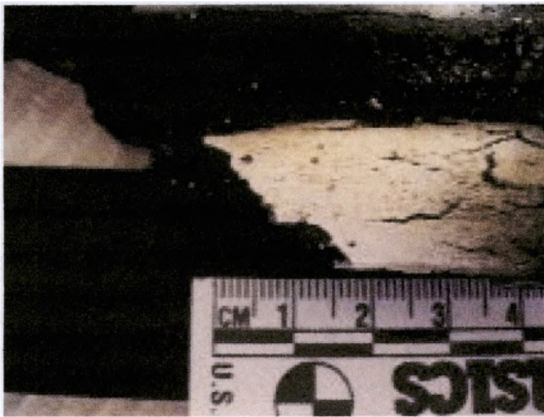


Figure 11. An Oblique Fracture



Figure 12. A Curved Fracture

Fracture Line



Figure 13. A Straight Fracture



Figure 14. A Wavy Fracture



Figure 15. A Saw-Like Fracture

Fracture Edge



Figure 16. A Sharp Fracture



Figure 17. A Dull Fracture

Fracture Depth



Figure 18. A Fracture with No Depth



Figure 19. A Fracture with 50% Depth

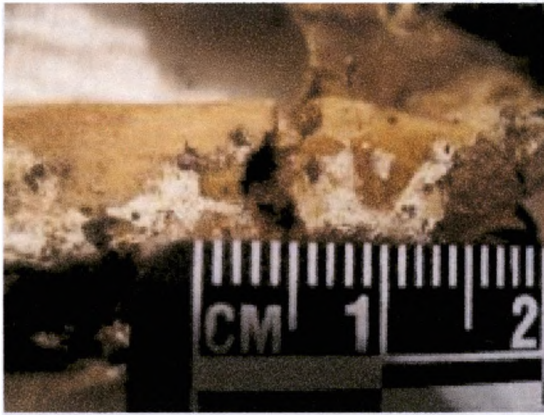


Figure 20. A Fracture with 75% Depth



Figure 21. A Fracture with 100% Depth

REFERENCES CITED

Binford, Lewis R.

1963 An Analysis of Cremations from Three Michigan Sites. *Wisconsin Archaeologist* 44:98-110.

Bohnert, Michael, Thomas Rost, Maria Faller-Marquardt, Dirk Ropohl, and Stefan Pollak.

1997 Fractures of the Base of the Skull in Charred Bodies: Post-Mortem Heat Injuries or Signs of Mechanical Traumatization? *Forensic Science International* 87:55-62.

Bonfield, W. and C.H. Li

1966 Deformation and Fracture of Bone. *Journal of Applied Physics* 37(2):869-875.

Buikstra, Jane E. and Mark Swegle

1989 Bone Modification Due to Burning: Experimental Evidence. *In Bone Modification*. Robson Bonnichsen and Marcella H. Sorg eds. Orono, Maine: Center for the Study of the First Americans. p. 247-258.

Daegling, David J., Jennifer Hotzman, Casey J. Self, and Michael Warren.

2006 Bone Fracture Mechanics: *In Vitro* Strain Gauge Analysis of the Ribs and Mandible During Failure. *Proceedings from the AAFS Annual Meeting* 2006. p. 315-316.

De Gruchy, Spencer and Tracy L. Rogers

2002 Identifying Chop Marks on Cremated Bone: A Preliminary Study. *Journal of Forensic Science* 47(5):933-936.

DiMaio, Vincent J. and Dominick DiMaio

2001 *Forensic Pathology*. Boca Raton, FL: CRC Press LLC.

Galloway, Alison

1999 Fracture Patterns and Skeletal Morphology: The Axial Skeleton. *In* Broken Bones: Anthropological Analysis of Blunt Force Trauma. Alison Galloway ed. Springfield, IL: Charles C. Thomas. p. 81-112.

Goff, M. Lee

1993 Estimation of the Postmortem Interval Using Arthropod Development and Successional Patterns. *Forensic Science Review* 81:81-94.

Gravetter, Frederick J. and Larry B. Wallnau

2007 Statistics for the Behavioral Sciences. Belmont, CA: Thomson Wadsworth.

Herrmann, Nicholas P. and Joanne L. Bennett

1999 The Differentiation of Traumatic and Heat-Related Fractures in Burned Bone. *Journal of Forensic Science* 44(3):461-469.

Hipp, John A. and Wilson C. Hayes

1998 Biomechanics of Fractures. *In* Skeletal Trauma: Fractures, Dislocations, Ligamentous Injuries. Bruce D. Browner et. al. eds. Philadelphia, PA: W.B. Saunders Company. p. 97-129.

Jackson, Daniel W.

2005 An Investigation into Identifying Sharp Force Trauma on Burned Bones. MA Thesis. Texas State University-San Marcos.

Kerley, Ellis R.

1965 The Microscopic Determination of Age in Human Bone. *American Journal of Physical Anthropology* 23:149-164.

Nelson, Russell

1992 A Microscopic Comparison of Fresh and Burned Bone. *Journal of Forensic Science* 37(4):1055-1060.

Piekarski, K.

1970 Fracture of Bone. *Journal of Applied Physics* 41(1):215-223.

Pope, Elayne J. and O'Brian C. Smith

2004 Identification of Traumatic Injury in Burned Cranial Bone: An Experimental Approach. *Journal of Forensic Science* 49(3):431-440.

Quatrehomme, Gerald, M. Bolla, M. Muller, J.P. Rocca, G. Grevin, P. Bailet, and A. Ollier.

1998 Experimental Single Controlled Study of Burned Bones: Contribution of Scanning Electron Microscopy. *Journal of Forensic Science* 43(2):417-422.

Thurman, M.D. and L.J. Wilmore.

1981 A Replicative Cremation Experiment. *North American Archaeologist* 2:275-283.

Tomczak, Paula D. and Jane E. Buikstra

1999 Analysis of Blunt Trauma Injuries: Verticle Deceleration Versus Horizontal Deceleration Injuries. *Journal of Forensic Science* 44(2):253-262.

VITA

Adam Holtan Richard was born in Mason City, Iowa, on June 14, 1980, to Gary and Sarah Richard. After graduating from Forest City High School in 1998, Adam enrolled at North Iowa Area Community College where he received an Associate of Arts and an Associate of Science degree in Biology. In 2000, Adam was accepted to Iowa State University where, two years later, he received a Bachelor of Science degree in Anthropology. During the summer of 2002, he took part in the Silver Creek Archaeological Research Project conducted by the University of Arizona. In 2005, after some time away from academics, Adam entered the Graduate College at Texas State University-San Marcos, and the next year, became a Student Affiliate of the American Academy of Forensic Sciences.

Permanent Address: 1021 Chestnut St.

Apt. B5

San Marcos, Texas 78666

This thesis was typed by Adam H. Richard.